

VNHC and Acrobot Title

Adan Moran-MacDonald, *Member, IEEE*, Manfredi Maggiore, *Member, IEEE**, and Xingbo Wang

Abstract—TODO: Abstract here.

Index Terms—TODO: keywords in alphabetical order, separated by commas.

I. INTRODUCTION

TODO: intro.

A. Notation

We use the following notation and terminology in this article. A matrix $A \in \mathbb{R}^{n \times m}$ is *right semi-orthogonal* if $AA^T = I_n$ and is *left semi-orthogonal* if $A^T A = I_m$. For $A \in \mathbb{R}^{n \times m}$ and $B \in \mathbb{R}^{p \times m}$, we define $[A; B] \in \mathbb{R}^{(n+p) \times m}$ as the matrix obtained by stacking A on top of B . For $T > 0$, the set of real numbers modulo T is denoted $[\mathbb{R}]_T$, with $[\mathbb{R}]_\infty := \mathbb{R}$. The gradient of a matrix-valued function $A : \mathbb{R}^m \rightarrow \mathbb{R}^{n \times n}$ is the block matrix of stacked partial derivatives, $\nabla_x A := [\frac{\partial A}{\partial x_1}; \dots; \frac{\partial A}{\partial x_m}] \in \mathbb{R}^{nm \times n}$. Given two matrices $A \in \mathbb{R}^{n \times m}$ and $B \in \mathbb{R}^{r \times s}$, the Kronecker product $A \otimes B \in \mathbb{R}^{nr \times ms}$ (see [1]) is the matrix

$$A \otimes B = \begin{bmatrix} A_{1,1}B & \cdots & A_{1,m}B \\ \vdots & \ddots & \vdots \\ A_{n,1}B & \cdots & A_{n,m}B \end{bmatrix}. \quad (1)$$

The Poisson bracket [2] between the functions $f(q, p)$ and $g(q, p)$ is

$$[f, g] := \sum_{i=1}^n \frac{\partial f}{\partial p_i} \frac{\partial g}{\partial q_i} - \frac{\partial f}{\partial q_i} \frac{\partial g}{\partial p_i}. \quad (2)$$

Finally, the Kronecker delta $\delta_i^j = 1$ if $i = j$ and 0 otherwise.

II. PROBLEM FORMULATION

In gymnastics terminology, a “giant” is the motion a gymnast performs to achieve full rotations around a horizontal bar [3]. A gymnast will begin by hanging at rest, then swing their legs appropriately to gain energy over time. The authors of [4] modelled the gymnast as a variable length pendulum, and studied how the pendulum’s length changes as a function of the gymnast’s limb angle. Labeling the pendulum length by r and the gymnast’s body orientation by θ , they observed experimentally that the value \dot{r}/r has the biggest impact on the

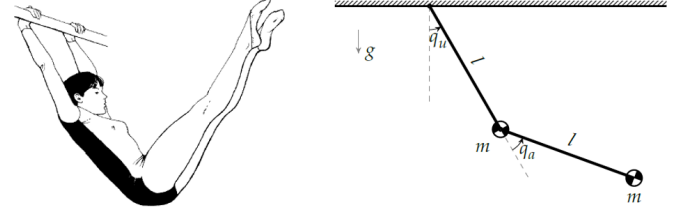


Fig. 1: The two-link acrobot as a model for a gymnast. Image modified from [6].

magnitude of energy injection. After testing several gymnasts under a variety of experimental conditions, they discovered that the peak value of \dot{r}/r occurred at the same fixed value of $\dot{\theta}/\theta$ for all gymnasts. In other words, gymnasts appear to move their legs as a function of their body angle and velocity when performing giants; doing so allows them to gain energy and rotate around the bar.

While the simplest model of a gymnast is the variable-length pendulum, a more realistic model is the two-link acrobot (Figure 1). Here, the top link represents the torso, while the bottom link represents the legs. The acrobot is actuated exclusively at the center joint (the hips). Controlling the acrobot is a nontrivial task because it is not feedback linearizable [5]. To solve the swingup problem, one might begin by designing a leg controller which provably injects energy into the acrobot, so that the resulting motion mimics that of a human performing a giant.

Previous attempts at acrobot giant generation have involved trajectory tracking, partial feedback linearization, or other energy-based methods (see [7]–[10]). While all these approaches succeed at making the acrobot rotate around the bar, none of them use the results of [4]. That is, none of these leg controllers track a function of the acrobot’s body angle and velocity. In 2016, Wang attempted to design such a controller [6] but was unable to prove the acrobot would gain energy over time. His approach was a rudimentary version of a recent technique know as the method of virtual nonholonomic constraints.

Virtual nonholonomic constraints (VNHCs) have been used for human-robot interaction [11]–[13], error-reduction on time-delayed systems [14], and they have shown marked improvements to the field of bipedal locomotion [15]–[17]. Indeed, they produce more robust walking motion in biped robots than other controllers which do not depend on velocity [18]. In particular, VNHCs may be capable of injecting and dissipating energy from a system in a robust manner, all while producing realistic biological motion.

In this article, we will design a virtual nonholonomic con-

Manuscript submitted for review on April 19, 2021.

A. Moran-MacDonald is with the Department of Electrical and Computer Engineering, University of Toronto, Toronto, ON, Canada (e-mail: adan.moran@mail.utoronto.ca).

M. Maggiore is with the Department of Electrical and Computer Engineering, University of Toronto, ON, Canada (e-mail: maggiore@control.utoronto.ca).

X. Wang is with ??? (e-mail: ???).

straint which provably injects energy into the acrobot through human-like giant motion.

MANFREDI: This section feels more like an intro than a problem formulation. Thoughts?

Before embarking on our design problem, let us summarize the relevant theory of VNHCS.

III. THEORY OF VNHCS

A. Simply Actuated Hamiltonian Systems

Take a mechanical system modelled with generalized coordinates $q = (q_1, \dots, q_n)$ on a configuration manifold $\mathcal{Q} = [\mathbb{R}]_{T_1} \times \dots \times [\mathbb{R}]_{T_n}$, where $T_i = 2\pi$ if q_i is an angle and $T_i = \infty$ if q_i is a displacement. The corresponding generalized velocities are $\dot{q} = (\dot{q}_1, \dots, \dot{q}_n) \in \mathbb{R}^n$.

Suppose this system has Lagrangian $\mathcal{L}(q, \dot{q}) = 1/2 \dot{q}^T D(q) \dot{q} - P(q)$, where the potential energy $P: \mathcal{Q} \rightarrow \mathbb{R}$ is smooth, and the inertia matrix $D: \mathcal{Q} \rightarrow \mathbb{R}^{n \times n}$ is smooth and positive definite for all $q \in \mathcal{Q}$. The conjugate of momentum to q is the vector $p := \partial \mathcal{L} / \partial \dot{q} = D(q) \dot{q} \in \mathbb{R}^n$. As per [2], the Hamiltonian of the system in (q, p) coordinates is

$$\mathcal{H}(q, p) = \frac{1}{2} p^T D^{-1}(q) p + P(q), \quad (3)$$

with dynamics

$$\begin{cases} \dot{q} = \nabla_p \mathcal{H}, \\ \dot{p} = -\nabla_q \mathcal{H} + B(q)\tau, \end{cases} \quad (4)$$

where $\tau \in \mathbb{R}^k$ is a vector of generalized input forces and the input matrix $B: \mathcal{Q} \rightarrow \mathbb{R}^{n \times k}$ is full rank for all $q \in \mathcal{Q}$. If $k < n$, we say the system is *underactuated* with degree of underactuation $(n - k)$.

It is easy to show using the matrix Kronecker product that (4) expands to

$$\begin{cases} \dot{q} = D^{-1}(q)p, \\ \dot{p} = -\frac{1}{2}(I_n \otimes p^T) \nabla_q D^{-1}(q)p - \nabla_q P(q) + B(q)\tau. \end{cases} \quad (5)$$

Because τ is transformed by $B(q)$, it is not obvious how any particular input force τ_i affects the system. As a first step in addressing this problem, we make the following assumptions.

Assumption 1: The input matrix $B(q) \equiv B \in \mathbb{R}^{n \times k}$ is constant, full rank, and $k < n$.

Assumption 2: There exists a right semi-orthogonal matrix $B^\perp \in \mathbb{R}^{(n-k) \times n}$ which is a left-annihilator for B .

Note that Assumption 2 requires the rows of B^\perp be unit vectors that are mutually orthogonal. When $k = (n - 1)$, Assumption 2 can be removed because it is automatically implied by Assumption 1.

The above assumptions allow us to define a canonical coordinate transformation of (3) which decouples the input forces. To define this transformation we will make use of the following lemma.

Lemma 1: Suppose Assumption 1 holds. Then there exists a nonsingular matrix $\hat{T} \in \mathbb{R}^{k \times k}$ so that the regular feedback transformation

$$\tau = \hat{T} \hat{\tau}$$

has a new input matrix \hat{B} for $\hat{\tau}$ which is left semi-orthogonal.

Proof: Since B is constant and full rank, it has a singular value decomposition $B = U^T \Sigma V$ where $\Sigma = [\text{diag}(\sigma_1, \dots, \sigma_k); \mathbf{0}_{(n-k) \times k}]$, $\sigma_i > 0$, and $U \in \mathbb{R}^{n \times n}$, $V \in \mathbb{R}^{k \times k}$ are unitary matrices [19]. Defining $T = \text{diag}(1/\sigma_1, \dots, 1/\sigma_k)$ and assigning the regular feedback transformation $\tau = VT\hat{\tau}$ yields a new input matrix $\hat{B} = BVT$ for $\hat{\tau}$ such that $\hat{B}^T \hat{B} = T^T \Sigma^T \Sigma T = I_k$. ■

In light of Lemma 1, there is no loss of generality in assuming that the input matrix is left semi-orthogonal. Now, let $\mathbf{B} := [B^\perp; B^T]$. Since B^\perp is a left annihilator of B and both B^\perp and B^T are right semi-orthogonal, one can easily show that \mathbf{B} is an orthogonal matrix.

Theorem 2: Take the Hamiltonian system (3) and suppose Assumptions 1 and 2 hold. The coordinate transformation $(\tilde{q} = \mathbf{B}q, \tilde{p} = \mathbf{B}p)$ is a canonical transformation and the resulting dynamics are given by

$$\begin{aligned} \mathcal{H}(\tilde{q}, \tilde{p}) &= \frac{1}{2} \tilde{p}^T M^{-1}(\tilde{q}) \tilde{p} + V(\tilde{q}), \\ \begin{cases} \dot{\tilde{q}} = M^{-1}(\tilde{q}) \tilde{p}, \\ \dot{\tilde{p}} = -\frac{1}{2}(I_n \otimes \tilde{p}^T) \nabla_{\tilde{q}} M^{-1}(\tilde{q}) \tilde{p} \\ \quad - \nabla_{\tilde{q}} V(\tilde{q}) + \begin{bmatrix} \mathbf{0}_{(n-k) \times k} \\ I_k \end{bmatrix} \tau, \end{cases} \end{aligned} \quad (6)$$

where $M^{-1}(\tilde{q}) := \mathbf{B}D^{-1}(\mathbf{B}^T \tilde{q})\mathbf{B}^T$ and $V(\tilde{q}) := P(\mathbf{B}^T \tilde{q})$.

Proof: Since \mathbf{B} is constant, this transformation satisfies $\partial \tilde{q}_i / \partial p_j = \partial \tilde{p}_i / \partial q_j = 0$ for all $i, j \in \{1, \dots, n\}$. This implies the Poisson brackets $[\tilde{q}_i, \tilde{q}_j]$ and $[\tilde{p}_i, \tilde{p}_j]$ are both zero. Then, since \mathbf{B} is orthogonal, $[\tilde{p}_i, \tilde{q}_j] = (\mathbf{B}_i)^T (\mathbf{B}^T)_j = \delta_i^j$. By (45.10) in [2], this is a canonical transformation and the new Hamiltonian is $\mathcal{H}(\mathbf{B}^T \tilde{q}, \mathbf{B}^T \tilde{p})$. Finally, since $\dot{\tilde{p}} = \mathbf{B} \dot{p}$, the input matrix for the system in (\tilde{q}, \tilde{p}) coordinates is $\mathbf{B}B = [\mathbf{0}_{(n-k) \times k}; I_k]$, which proves the theorem. ■

We call the (\tilde{q}, \tilde{p}) coordinates *simply actuated coordinates*. The first $(n - k)$ configuration variables in \tilde{q} , labelled q_u , are the *unactuated coordinates*; the remaining k configuration variables, labelled q_a , are the *actuated coordinates*. The corresponding (p_u, p_a) in \tilde{p} are the *unactuated* and *actuated momenta*, respectively.

B. Virtual Nonholonomic Constraints

Griffin and Grizzle [15] were the first to define relative degree two nonholonomic constraints which can be enforced through state feedback. Horn et. al later extended their results [16] to derive the constrained dynamics for a certain class of mechanical systems.

These researchers made use of the unactuated conjugate of momentum, but they developed their results in the Lagrangian framework. In particular, they focused on Lagrangian systems with degree of underactuation one. In this section we reformulate their ideas into the Hamiltonian framework and extend the definition of a virtual nonholonomic constraint to systems with higher degree of underactuation. This reformulation will provide us with better intuition and a more explicit form of the constrained dynamics.

For the rest of this section we take the system of inquiry to be a Hamiltonian mechanical system in simply actuated

coordinates, as in (6). For simplicity of notation, we relabel (\tilde{q}, \tilde{p}) to (q, p) .

Definition 3: A *virtual nonholonomic constraint* (VNHC) of order k is a relation $h(q, p) = 0$ where $h : \mathcal{Q} \times \mathbb{R}^n \rightarrow \mathbb{R}^k$ is C^2 , $\text{rank}([dh_q, dh_p]) = k$ for all $(q, p) \in h^{-1}(0)$, and there exists a feedback controller $\tau(q, p)$ rendering the *constraint manifold* Γ invariant, where

$$\Gamma = \{(q, p) \mid h(q, p) = 0, dh_q \dot{q} + dh_p \dot{p} = 0\}. \quad (7)$$

The constraint manifold is a $2(n - k)$ -dimensional closed embedded submanifold of $\mathcal{Q} \times \mathbb{R}^n$. A VNHC thereby allows us to study a reduced-order model of the system: it reduces the original $2n$ differential equations to $2(n - k)$ equations. In particular, if $k = (n - 1)$, the constraint manifold is *always* 2-dimensional and its dynamics can be plotted on a plane.

We often want to stabilize a constraint within some neighbourhood of Γ . To see when this is possible, let us define the error output $e = h(q, p)$. If any component of e_i has relative degree 1, we may not be able to stabilize Γ – we can always guarantee $e_i \rightarrow 0$, but not necessarily $\dot{e}_i \rightarrow 0$. It is for this reason that we define the following special type of VNHC.

Definition 4: A VNHC $h(q, p) = 0$ of order k is *regular* if the output $e = h(q, p)$ is of relative degree $\{2, 2, \dots, 2\}$ everywhere on the constraint manifold Γ .

The authors of [15], [16] observed that relations which use only the unactuated conjugate of momentum often have vector relative degree $\{2, \dots, 2\}$. Indeed, we shall now provide a characterization of regularity which shows that regular constraints cannot use the actuated momentum at all.

To ease notation in the rest of this section, we use the following shorthand:

$$\mathcal{A}(q, p_u) := dh_q(q, p_u)M^{-1}(q), \quad (8)$$

$$\mathcal{M}(q, p) := (I_{n-k} \otimes p^T) \nabla_{q_u} M^{-1}(q). \quad (9)$$

Theorem 5: A relation $h(q, p) = 0$ for system (6) is a regular VNHC of order k if and only if $dh_{p_a} = \mathbf{0}_{k \times k}$ and

$$\text{rank} \left((\mathcal{A}(q, p_u) - dh_{p_u} \mathcal{M}(q, p)) \begin{bmatrix} \mathbf{0}_{(n-k) \times k} \\ I_k \end{bmatrix} \right) = k,$$

everywhere on the constraint manifold Γ .

Proof: Let $e = h(q, p) \in \mathbb{R}^k$. If $dh_{p_a} \neq \mathbf{0}_{k \times k}$ for some $(q, p) \in \Gamma$, then τ appears in \dot{e} and the VNHC is not of relative degree $\{2, \dots, 2\}$. Suppose now that $dh_{p_a} = \mathbf{0}_{k \times k}$. Then $\dot{e} = \mathcal{A}(q, p_u)p - dh_{p_u} (1/2 \mathcal{M}(q, p)p + \nabla_{q_u} V(q))$. Taking one further derivative provides $\ddot{e} = (\star) - dh_{p_u} (1/2 d/dt (\mathcal{M}(q, p)p)) + \mathcal{A}(q, p_u)[\mathbf{0}_{(n-k) \times k}; I_k]\tau$, where (\star) is a continuous function of q and p . One can further show that $dh_{p_u} (1/2 d/dt (\mathcal{M}(q, p)p)) = (\star) + dh_{p_u} \mathcal{M}(q, p)[\mathbf{0}_{(n-k) \times k}; I_k]\tau$. Hence,

$$\ddot{e} = (\star) + (\mathcal{A}(q, p_u) - dh_{p_u} \mathcal{M}(q, p)) \begin{bmatrix} \mathbf{0}_{(n-k) \times k} \\ I_k \end{bmatrix} \tau,$$

which we write as $\ddot{e} = E(q, p) + H(q, p)\tau$ for appropriate E and H . From the definition of regularity, the VNHC h is regular when e is of relative degree $\{2, \dots, 2\}$, which is true if and only if the matrix premultiplying τ is nonsingular, and hence that H is invertible. This proves the theorem. ■

Under additional mild conditions (see [20]), a regular VNHC of order k can be stabilized by the output-linearizing phase-feedback controller

$$\tau(q, p) = -H^{-1}(q, p) (E(q, p) + k_p e + k_d \dot{e}), \quad (10)$$

where $k_p, k_d > 0$ are control parameters which can be tuned on the resulting error dynamics $\ddot{e} = -k_p e - k_d \dot{e}$.

In Section IV we will enforce a regular constraint on the acrobot of the form $h(q, p) = q_a - f(q_u, p_u)$, where the actuators track a function of the unactuated variables. Intuitively then, the constrained dynamics should be parameterized by (q_u, p_u) . Unfortunately, \dot{q}_u depends on p_a , and for general systems one cannot solve explicitly for p_a in terms of (q_u, p_u) because the \dot{p} dynamics contains the coupling term $(I_n \otimes p^T) \nabla_q M(q)p$.

We now introduce an assumption which allows us to solve for p_a as a function of (q_u, p_u) , which in turn allows us to find the constrained dynamics.

Assumption 3: The inertia matrix does not depend on the unactuated coordinates, so that $\nabla_{q_u} M(q) = \mathbf{0}_{n(n-k) \times n}$.

Theorem 6: Let \mathcal{H} be a mechanical system in simply actuated coordinates satisfying Assumption 3. Let $h(q, p_u) = 0$ be a regular VNHC of order k with constraint manifold Γ . Suppose that on Γ one can solve for q_a as a function $q_a = f(q_u, p_u)$. Then the constrained dynamics are given by

$$\begin{aligned} \dot{q}_u &= [I_{(n-k)} \quad \mathbf{0}_{(n-k) \times k}] M^{-1}(q)p \\ \dot{p}_u &= -\nabla_{q_u} V(q) \end{aligned} \quad \left| \begin{array}{l} q_a = f(q_u, p_u) \\ p_a = g(q_u, p_u) \end{array} \right. \quad (11)$$

where

$$\begin{aligned} g(q_u, p_u) &:= (\mathcal{A}(q, p_u)[\mathbf{0}_{(n-k) \times k}; I_k])^{-1} (dh_{p_u} \nabla_{q_u} V(q) \\ &\quad - \mathcal{A}(q, p_u)[I_{(n-k)}; \mathbf{0}_{k \times (n-k)}]p_u)|_{q_a=f(q_u, p_u)}. \end{aligned} \quad (12)$$

Proof: Setting $e = h(q, p_u)$ and using Assumption 3, we find that $\dot{e} = \mathcal{A}(q, p_u)p - dh_{p_u} \nabla_{q_u} V(q)$. Notice that $\mathcal{A}(q, p_u)p = \mathcal{A}(q, p_u)[\mathbf{0}_{(n-k) \times k}; I_k]p_a + \mathcal{A}(q, p_u)[I_{(n-k)}; \mathbf{0}_{k \times (n-k)}]p_u$. Since $h(q, p_u)$ is regular, $\mathcal{A}(q, p_u)$ is invertible. Taking $e = \dot{e} = 0$, solving for p_a , and setting $q_a = f(q_u, p_u)$ completes the proof. ■

We conclude this section by formalizing the notion of energy injection for VNHCs.

Definition 7: Let \mathcal{Q} be an n -dimensional smooth generalized cylinder. Let $f : \mathcal{Q} \rightarrow \mathcal{Q} \times \mathbb{R}^n$ be a smooth vector field and let $D \subset M$ be open. The system described by $\dot{x} = f(x)$ *gains energy on D* if, for all compact sets $K \subset D$ and for almost every initial condition $x(0) \in K$, there exists $T > 0$ such that $x(t) \notin K$ ($\forall t > T$). The system *loses energy on D* if it gains energy in negative-time.

Any system satisfying Definition 7 can have unstable equilibria on D , but not limit cycles nor closed orbits. The next definition ties this notion of energy gain to VNHCs.

Definition 8: A regular VNHC $h(q, p) = 0$ with constraint manifold Γ *injects (dissipates) energy on $D \subset \Gamma$* if the constrained dynamics gain (lose) energy everywhere on D , except possibly on a set of measure zero.

Comparison with existing literature: Horn et.al. provide the constrained dynamics for VNHCs in [18]. Their assumption **H2** is what we call regularity, and our requirement that one can solve for $q_a = f(q_u, p_u)$ on Γ implies their assumption

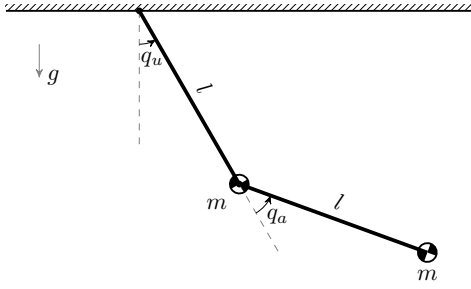


Fig. 2: A simple acrobot has massless rods of equal length l and equal masses m at the tips.

H3 holds true. The only real distinction between this section and their work is that our constrained dynamics are explicit functions of the Hamiltonian phase coordinates (q_u, p_u) . In fact, our constrained dynamics (11) coincide with their system (17) when one chooses the special case $\theta_1 = q_u$ and $\theta_2 = p_u$. This explicit representation will be beneficial when we apply the theory of VNHCs to the acrobot.

IV. THE ACROBOT VNHC

Our goal in this article is to design a VNHC which injects energy into the acrobot through giant-like motion. We will use the simplified acrobot model in Figure 2, where we assume the torso and leg rods are of equal length l with equal point masses m at the tips. A real gymnast cannot swing their legs in full circles, though they are usually flexible enough to raise them parallel to the floor; hence, we assume the leg angle q_a lies in $[-Q_a, Q_a]$ for some $Q_a \in [\frac{\pi}{2}, \pi]$. We also ignore any frictional forces.

The acrobot has inertia matrix M , potential function V (with respect to the horizontal bar), and input matrix B given as follows:

$$M(q) = \begin{bmatrix} ml^2(3 + 2\cos(q_a)) & ml^2(1 + \cos(q_a)) \\ ml^2(1 + \cos(q_a)) & ml^2 \end{bmatrix}, \quad (13)$$

$$V(q) = -mgl(2\cos(q_u) + \cos(q_u + q_a)), \quad (14)$$

$$B = [0; 1]. \quad (15)$$

The conjugate of momenta is $p = (p_u, p_a) = M(q)\dot{q}$. The dynamics of the acrobot in (q, p) coordinates are given in (16), where for shorthand, we write $c_u := \cos(q_u)$, $c_a := \cos(q_a)$, and $c_{ua} := \cos(q_u + q_a)$; likewise, $s_u := \sin(q_u)$, $s_a := \sin(q_a)$, and $s_{ua} := \sin(q_u + q_a)$.

$$\begin{aligned} \mathcal{H}(q, p) &= \frac{1}{2}p^\top M^{-1}(q)p - mgl(2c_u + c_{ua}), \\ \begin{cases} \dot{q} &= M^{-1}(q)p, \\ \dot{p}_u &= -mgl(2s_u + s_{ua}), \\ \dot{p}_a &= -\frac{1}{2}p^\top \nabla_{q_a} M^{-1}(q)p - mgl s_{ua} + \tau, \end{cases} \end{aligned} \quad (16)$$

The control input is a force $\tau \in \mathbb{R}$ affecting only the dynamics of p_a , representing a torque acting on the hip joint. This means (q, p) are simply actuated coordinates in the phase space $\mathcal{Q} \times \mathcal{P}$ where $\mathcal{Q} = \mathbb{S}^1 \times \mathbb{S}^1$, and $\mathcal{P} = \mathbb{R} \times \mathbb{R}$. We can therefore apply the theory from Section III to design a VNHC of the form $q_a = f(q_u, p_u)$. Since we need the VNHC to be regular, the following proposition will be useful.

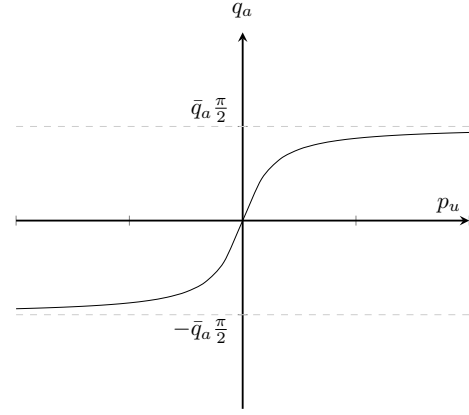


Fig. 3: The acrobot constraint $q_a = \bar{q}_a \arctan(I p_u)$.

Proposition 9: A relation $h(q, p) = q_a - f(p_u) = 0$ with $f \in C^2(\mathbb{R}; \mathbb{S}^1)$ is a regular VNHC of order 1 for the acrobot.

Proof: The regularity matrix for the acrobot evaluates to $((1 + c_a)\partial_{q_u}f(q_u, p_u) + (3 + 2c_a))/(ml^2(2 - c_a^2))$. Since $\partial_{q_u}f = 0$, this matrix is strictly positive for all values of q_a , and hence is full rank everywhere on the constraint manifold. ■

To design our VNHC, we begin by examining a person on a seated swing. The person extends their legs when the swing moves forwards, and retracts their legs when the swing moves backwards. As the swing gains speed, the person leans their body while extending their legs higher, thereby shortening the distance from their center of mass to the pivot and adding more energy to the swing [21].

Now imagine the person's torso is affixed to the swing's rope so they are always upright. Imagine further that the swing has no seat at all, allowing the person to extend their legs beneath them. This position is identical to that of a gymnast on a bar.

The acrobot's legs are rigid rods which cannot retract, so we emulate the person on a swing by pivoting the legs toward the direction of motion. Since a person lifts their legs higher at higher speeds, the acrobot's legs should pivot to an angle proportional to the swing's speed. Because the direction of motion is entirely determined by p_u , one VNHC which emulates this process is $q_a = \bar{q}_a \arctan(I p_u)$, displayed in Figure 3. Here, $\bar{q}_a \in]0, 2Q_a/\pi]$ is constant and $I \in \mathbb{R}$ is a fixed control parameter.

This constraint does not perfectly recreate giant motion, during which the gymnast's legs are almost completely extended [3]. It instead pivots the legs partially during rotations. However, the behaviour looks similar enough that this constraint will still inject energy into the acrobot. Our final VNHC is

$$h(q, p) = q_a - \bar{q}_a \arctan(I p_u). \quad (17)$$

Recall that (q_u, p_u) denote the angle and momentum of the acrobot's torso. By Theorem 6, the constrained acrobot is parameterized fully by $(q_u, p_u) \in \mathbb{S}^1 \times \mathbb{R}$. It is easy to show that the constrained dynamics are just the torso dynamics

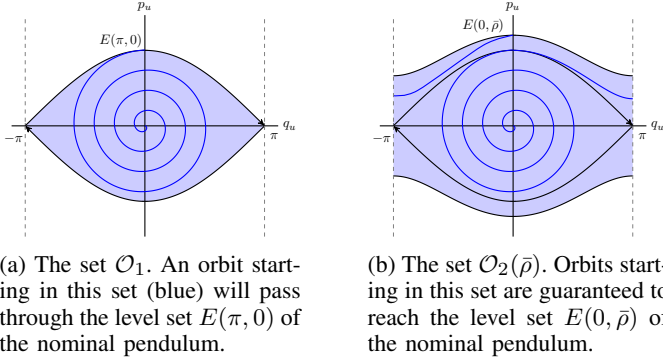


Fig. 4: The sets on which the acrobot gains energy, according to Theorem 10.

obtained when one swings the legs according to (17):

$$\begin{cases} \dot{q}_u = \frac{(1+I^2 p_u^2) p_u + m^2 g l^3 \bar{q}_a I (2s_u + s_{ua})(1+c_a)}{m l^2 (1+I^2 p_u^2)(3+2c_a)}, \\ \dot{p}_u = -m g l (2s_u + s_{ua}), \end{cases} \quad (18)$$

subject to $q_a = \bar{q}_a \arctan(I p_u)$.

Suppose for a moment that $I = 0$, i.e. that the legs stay fully extended. The acrobot becomes a nominal pendulum with two masses, whose total mechanical energy is

$$E(q_u, p_u) := \frac{p_u^2}{10m l^2} + 3m g l (1 - \cos(q_u)). \quad (19)$$

The upright equilibrium of this pendulum is located at $(q_u, p_u) = (\pi, 0)$. Imagine the pendulum hits the bottom of the swing arc with momentum $p_u \neq 0$. To reach the upright equilibrium, this momentum must be $p_u = \pm \sqrt{60m^2 g l^3}$ because $E(\pi, 0) = E(0, \pm \sqrt{60m^2 g l^3})$. If the momentum is smaller in magnitude, the acrobot will oscillate; if it is larger, the pendulum will rotate around the bar.

When the pendulum is oscillating, its phase (q_u, p_u) lies in the set

$$\mathcal{O}_1 := \{(q_u, p_u) \in \mathbb{S}^1 \times \mathbb{R} \mid E(q_u, p_u) < E(\pi, 0)\}, \quad (20)$$

which is shown in Figure 4a. If for some $I \neq 0$ our VNHC injects energy into the acrobot on \mathcal{O}_1 , and the constrained dynamics escape \mathcal{O}_1 in finite time, then the acrobot is guaranteed to perform giant-like motion and begin rotating around the bar.

When the pendulum is rotating with bounded momentum $|p_u| < \bar{\rho}$ (for some chosen $\bar{\rho}$), the phase must lie inside the rotation domain

$$\mathcal{R}(\rho) := \{(q_u, p_u) \in \mathbb{S}^1 \times \mathbb{R} \mid E(\pi, 0) < E(q_u, p_u) < E(0, \rho)\}. \quad (21)$$

Connecting the regions (20) and (21) yields the set

$$\mathcal{O}_2(\bar{\rho}) := \{(q_u, p_u) \in \mathbb{S}^1 \times \mathbb{R} \mid E(q_u, p_u) < E(0, \bar{\rho})\}, \quad (22)$$

shown in Figure 4b. If the VNHC injects energy on $\mathcal{O}_2(\bar{\rho})$ for some $I \neq 0$, then the acrobot must necessarily swing up, begin rotating, and eventually rotate with a momentum of at least $\bar{\rho}$.

Unfortunately, our VNHC does not always inject energy on \mathcal{O}_1 and $\mathcal{O}_2(\bar{\rho})$. If I is too large, the leg controller saturates and

the body oscillates without gaining energy. Choosing I small enough guarantees the legs will synchronize properly with the body, and the acrobot will begin rotating around the bar. The following theorem provides conditions under which such an I exists.

Theorem 10: Consider the acrobot with Hamiltonian dynamics as in (16).

- 1) For any m, g, l, \bar{q}_a , there exists $I^* > 0$ such that, for all $I \in]0, I^*]$, the VNHC (17) injects energy into the acrobot on \mathcal{O}_1 . Moreover, almost every orbit will escape the closure of \mathcal{O}_1 in finite time. If instead $I \in [-I^*, 0[$, the VNHC dissipates energy.
- 2) Let $C = m^2 g l^3 \bar{q}_a$ and define $b : \mathbb{S}^1 \times \mathbb{R}_{>0} \rightarrow \mathbb{R}$ by

$$b(\beta, \rho_0) := \frac{5C \left(\frac{C}{\bar{q}_a} \left(18s_\beta^2 + 30c_\beta(1 - c_\beta) \right) - c_\beta \rho_0^2 \right)}{|\rho_0| \sqrt{\rho_0^2 - 30m^2 g l^3 (1 - c_\beta)}}.$$

Define $S(\rho_0) := \int_0^{2\pi} b(\sigma, \rho_0) d\sigma$. Fix $\bar{\rho} > \sqrt{60m^2 g l^3}$ and suppose there exists $\epsilon > 0$ so that $S(\rho_0) \geq \epsilon$ for all $\rho_0 \in [\sqrt{60m^2 g l^3}, \bar{\rho}]$. Then there exists $I^{**} \in]0, I^*]$ such that, for all $I \in]0, I^{**}]$, the VNHC (17) injects energy into the acrobot on $\mathcal{O}_2(\bar{\rho})$. If instead $I \in [-I^{**}, 0[$, the VNHC dissipates energy.

Proof: See Section VI. ■

Notice that $\mathcal{O}_1 \subset \mathcal{O}_2(\bar{\rho})$, yet Theorem 10 considers these sets separately. This separation is advantageous because the first result holds for any m, g, l , and \bar{q}_a . In other words, the first result of Theorem 10 states that all acrobots constrained by (17) will gain enough energy to begin rotating around the bar.

For the acrobot to achieve giants with energy $E(0, \bar{\rho})$, it must satisfy the assumption on the integral of $b(\beta, \rho_0)$. The value of this integral depends on the acrobot's physical parameters. If the assumption holds, there is some control value I (which depends on $\bar{\rho}$) for which the acrobot will achieve rotations with a momentum of at least $\bar{\rho}$.

V. EXPERIMENTAL RESULTS

We tested our VNHC on the physical acrobot built by Xingbo Wang [6] (Figure 5). The torso and legs on this robot have differing masses and lengths, so its inertia matrix and potential function are **not** described by (13)-(14). If our VNHC injects energy into this acrobot, then we can infer that VNHCs are robust to model mismatch.

For our VNHC to inject energy, we know the control parameter I must be small (as per Theorem 10), but it must also be large enough to overcome friction in leg motor. Setting $\bar{q}_a = 1$, we experimentally determined that $I = 10$ is sufficient to ensure the actuator can fully rotate in its allowable range $q_a \in [-\frac{\pi}{2}, \frac{\pi}{2}]$. This is the value of I we used in all simulations and experiments.

A. Simulations Results

Evaluating the true mechanical energy of Wang's acrobot at the VNHC $q_a = 0$ yields the energy of the nominal pendulum,

$$E(q_u, p_u) \approx 396.5501 p_u^2 + 0.5997(1 - \cos(q_u)).$$



Fig. 5: The acrobot built by Wang [6].

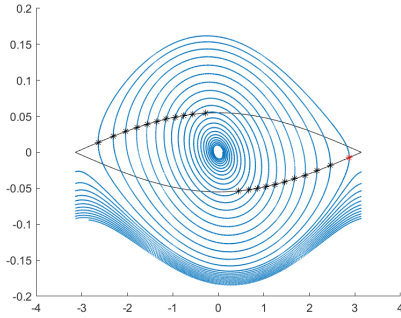


Fig. 6: A simulated orbit of Wang's acrobot.

We simulated Wang's acrobot with initial condition $(q_u, p_u) = (\pi/32, 0)$ and plotted the resulting orbit in Figure 6.

The set $E_\pi := E(\pi, 0)$ is outlined in black. Due to the model mismatch, E_π is no longer the boundary between rotations and oscillations. The oscillation domain is actually much larger: orbits rotate once they hit the p_u -axis at $|p_u| \approx 0.15$, while E_π intersects the p_u -axis at $|p_u| \approx 0.055$. Despite this, the VNHC still injects energy into the acrobot. The points where the orbit exits E_π are marked with black stars, with the final departure marked by a red star. After this final departure, the acrobot begins rotating and continues to gain energy over time.

To verify numerically that the acrobot would consistently achieve rotations, we ran a Monte-Carlo simulation [22] where we initialized the acrobot randomly inside the sublevel set

$$\left\{ (q_u, p_u) \in \mathbb{S}^1 \times \mathbb{R} \mid E(q_u, p_u) \leq E\left(\frac{\pi}{32}, 0\right) \right\},$$

and measured the how long it took to begin rotating. The results in Figure 7 show that the acrobot always rotated within 10–35 seconds.

B. Physical Experiments

Wang's acrobot has an encoder which measures q_u and \dot{q}_u . Additionally, the leg actuator is a servo motor with a built-in PID controller which provides measurements of q_a . To implement our VNHC, we estimated \dot{q}_a through sequential values of q_a and computed p_u through $p_u = e_1^T M(q)\dot{q}$. We

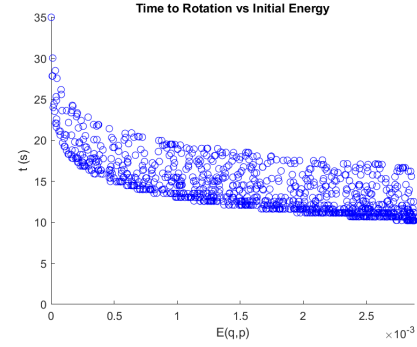
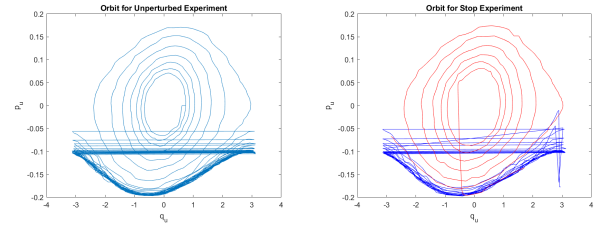


Fig. 7: Monte Carlo simulation results.



(a) The baseline test. (b) Acrobot orbit before (blue) and after (red) stopping.

Fig. 8: The physical acrobot's orbit during baseline and stop tests.

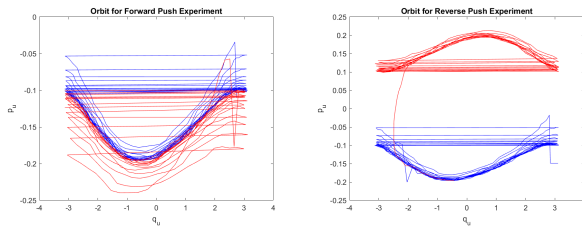
directly assigned the actuator setpoint at iteration $k \in \mathbb{Z}_{>0}$ via $q_a^k = \arctan(10p_u^{k-1})$. We then performed the following tests.

- 1) **Baseline Test:** we initialized the acrobot at $(q_u, p_u) \approx (\pi/8, 0)$. The resulting orbit is shown in Figure 8a; the acrobot is clearly gaining energy over time.
- 2) **Stop Test:** we initialized the acrobot at $(q_u, p_u) \approx (\pi, 0)$, let it run for 15 seconds, then stopped it at the bottom of its arc. The resulting orbit is shown in Figure 8b. The blue curves correspond to the orbit before the disturbance, while the red spiral confirms that the acrobot begins oscillating after it is stopped. Despite the disturbance, it gains energy and eventually starts rotating again.
- 3) **Push Test:** to see how the acrobot responds when pushed, we allowed the acrobot to rotate undisturbed for 15 seconds and then pushed it in its direction of motion. The orbit in Figure 9a shows that the acrobot speeds up to rotate with energy $E(0, -0.22)$, but then slows down until it reaches a rotation with energy $E(0, -0.195)$. We repeated this test by pushing the acrobot against its direction of motion. The orbit in Figure 9b demonstrates that the acrobot responds by readily changing direction, and quickly achieves its maximum speed with energy $E(0, 0.195)$.

These push tests suggest that our VNHC injects energy into Wang's acrobot on $\mathcal{O}_2(0.195)$.

C. Summary of Results

These simulations and experiments demonstrate that VNHCs are excellent tools for injecting energy. In particular,



(a) The forwards push test.

(b) The reverse push test.

Fig. 9: The acrobot orbit before (blue) and after (red) pushing.

energy injection through VNHCs appears to be robust against a variety of disturbances, including significant model mismatch.

VI. PROOF OF THEOREM 10

VII. CONCLUSION

In this article we summarized the existing theory of virtual nonholonomic constraints (VNHCs) **TODO conclude nicely** In the end, we demonstrated that virtual nonholonomic constraints are capable of injecting and dissipating energy in a robust manner, all while producing realistic biological motion.

REFERENCES

- [1] R. D. Schafer, *An Introduction to Non-Associative Algebras*. New York: Dover Publications, 1996.
- [2] L. D. Landau and E. M. Lifschitz, *Mechanics*, 3rd ed. Butterworth-Heinemann, January 1982.
- [3] P. E. Pidcoe, "The biomechanics principles behind training giant swings," Online, Virginia Commonwealth University, Richmond, VA, USA, August 2005, accessed 11 September 2020. <https://us-agym.org/pages/home/publications/technique/2005/8/giant.pdf>.
- [4] V. Sevez, E. Berton, G. Rao, and R. J. Bootsma, "Regulation of pendulum length as a control mechanism in performing the backward giant circle in gymnastics," *Human Movement Science*, vol. 28, no. 2, pp. 250 – 262, March 2009.
- [5] J. Hauser and R. Murray, "Nonlinear controllers for non-integrable systems: the acrobot example," in *1990 American Control Conference*. San Diego, USA: IEEE, May 1990.
- [6] X. Wang, "Motion control of a gymnastics robot using virtual holonomic constraints," Master's thesis, University of Toronto, 2016.
- [7] E. Papadopoulos and G. Papadopoulos, "A novel energy pumping strategy for robotic swinging," in *2009 17th Mediterranean Conference on Control and Automation*. Thessaloniki, Greece: IEEE, June 2009.
- [8] T. Henmi, M. Chujo, Y. Ohta, and M. Deng, "Reproduction of swing-up and giant swing motion of acrobot based on a technique of the horizontal bar gymnast," in *Proceedings of the 11th World Congress on Intelligent Control and Automation*. Shenyang, China: IEEE, June 2014.
- [9] X. Zhang, H. Cheng, Y. Zhao, and B. Gao, "The dynamical servo control problem for the acrobot based on virtual constraints approach," in *The 2009 IEEE/RSJ International Conference on Intelligent Robots and Systems*. St. Louis, USA: IEEE, October 2009.
- [10] K. Ono, K. Yamamoto, and A. Imadu, "Control of giant swing motion of a two-link horizontal bar gymnastic robot," *Advanced Robotics*, vol. 15, no. 4, pp. 449 – 465, 2001.
- [11] T. Takubo, H. Arai, and K. Tanie, "Virtual nonholonomic constraint for human-robot cooperation in 3-d space," in *2000 IEEE/RSJ International Conference on Intelligent Robots and Systems*. Takamatsu, Japan: IEEE, October 2000.
- [12] S. Shibata and T. Murakami, "Psd based virtual nonholonomic constraint for human interaction of redundant manipulator," in *Proceedings of the 2004 IEEE International Conference on Control Applications*. Taipei, Taiwan: IEEE, September 2004.
- [13] J. D. Castro-Díaz, P. Sánchez-Sánchez, A. Gutiérrez-Giles, M. Arteaga-Pérez, and J. Pliego-Jiménez, "Experimental results for haptic interaction with virtual holonomic and nonholonomic constraints," *IEEE Access*, vol. 8, pp. 120959 – 120973, July 2020.
- [14] S. Vozar, Z. Chen, P. Kazanzides, and L. L. Whitcomb, "Preliminary study of virtual nonholonomic constraints for time-delayed teleoperation," in *2015 IEEE/RSJ International Conference on Intelligent Robots and Systems*. Hamburg, Germany: IEEE, October 2015.
- [15] B. Griffin and J. Grizzle, "Nonholonomic virtual constraints for dynamic walking," in *2015 54th IEEE Conference on Decision and Control*. Osaka, Japan: IEEE, December 2015.
- [16] J. Horn, A. Mohammadi, K. Hamed, and R. Gregg, "Hybrid zero dynamics of bipedal robots under nonholonomic virtual constraints," *IEEE Control Systems Letters*, vol. 3, no. 2, pp. 386 – 391, April 2019.
- [17] W. K. Chan, Y. Gu, and B. Yao, "Optimization of output functions with nonholonomic virtual constraints in underactuated bipedal walking control," in *2018 Annual American Control Conference*. Milwaukee, USA: IEEE, June 2018.
- [18] J. C. Horn, A. Mohammadi, K. A. Hamed, and R. D. Gregg, "Non-holonomic virtual constraint design for variable-incline bipedal robotic walking," *IEEE Robotics and Automation Letters*, vol. 5, pp. 3691 – 3698, February 2020.
- [19] G. Golub and W. Kahan, "Calculating the singular values and pseudo-inverse of a matrix," *Journal of the Society for Industrial and Applied Mathematics: Series B, Numerical Analysis*, vol. 2, no. 2, pp. 204–224, 1965.
- [20] M. Maggiore and L. Consolini, "Virtual holonomic constraints for euler-lagrange systems," *IEEE Transactions on Automatic Control*, vol. 58, no. 4, pp. 1001 – 1008, April 2013.
- [21] S. Wirkus, R. Rand, and A. Ruina, "How to pump a swing," *The College Mathematics Journal*, vol. 29, no. 4, pp. 266 – 275, 1998.
- [22] N. Metropolis, "The beginning of the monte carlo method," *Los Alamos Science*, pp. 125–130, 1987, 1987 special issue dedicated to Stanislaw Ulam.